

Pressure effects on Jahn-Teller distortion in perovskites: The roles of local and bulk compressibilities

Fernando Aguado and Fernando Rodríguez*

MALTA Consolider Team, Departamento de Ciencias de la Tierra y Física de la Materia Condensada (DCITIMAC), Facultad de Ciencias, Universidad de Cantabria, 39005 Santander, Spain

Rafael Valiente

MALTA Consolider Team, Departamento Física Aplicada, Facultad de Ciencias, Universidad de Cantabria, 39005 Santander, Spain

Jean-Paul Itié

Synchrotron SOLEIL, L'Orme des Merisiers, St Aubin BP48, 91192 Gif-sur-Yvette cedex, France

Michael Hanfland

European Synchrotron Radiation Facility (ESRF), BP220, 156 rue des Martires, 38043 Grenoble Cedex, France

(Received 21 October 2011; revised manuscript received 24 February 2012; published 26 March 2012)

The interplay between the Jahn-Teller (JT) effect and octahedron tilting in transition-metal perovskites is investigated as a function of pressure. Our focus is on its effects on the exchange and electron-phonon interactions, both having a strong influence on materials properties. We demonstrate that the JT distortion in Cu^{2+} and Mn^{3+} is reduced upon compression and is eventually suppressed at pressures above 20 GPa. X-ray diffraction and x-ray absorption measurements in A_2CuCl_4 layer perovskites (A: Rb, $\text{C}_n\text{H}_{2n+1}\text{NH}_3$; $n = 1-3$) show that, although pressure slightly reduces the long Cu-Cl distance in comparison to the Cu-Cu distance in the layer, the JT distortion is stable in the 0–20 GPa range. The difference between lattice ($\beta_0^C = 0.14 \text{ GPa}^{-1}$) and local CuCl_6 ($\beta_0 = 0.016 \text{ GPa}^{-1}$) compressibilities, together with the high stability of the JT distortion, lead to CuCl_6 tilts upon compression. The evolution of the elongated CuCl_6 octahedron in A_2CuCl_4 , as well as MnF_6 in CsMnF_4 and MnO_6 in LaMnO_3 and DyMnO_3 , toward a nearly regular octahedron takes place above 20 GPa, in agreement with experimental results and a model analysis based on the JT energy derived from optical absorption spectroscopy: $E_{\text{JT}} = 0.25-0.45 \text{ eV/Cu}^{2+}$, $E_{\text{JT}} = 0.45 \text{ eV/Mn}^{3+}$ (CsMnF_4), and $E_{\text{JT}} = 0.25 \text{ eV/Mn}^{3+}$ (LaMnO_3). The proposed model clarifies controversial results about pressure-induced JT quenching in Cu^{2+} and Mn^{3+} systems, providing an efficient complementary means to predict pressure behavior in perovskites containing JT transition-metal ions.

DOI: [10.1103/PhysRevB.85.100101](https://doi.org/10.1103/PhysRevB.85.100101)

PACS number(s): 71.70.Ej, 61.05.cj, 61.50.Ks, 64.30.-t

Transition-metal perovskites display an ample variety of structures with relevant physical phenomena, having a deep impact in materials science,^{1,2} applied physics,^{3,4} and geophysics.^{5,6} The interplay between the local structure and the exchange couplings between octahedral transition-metal ions governs materials properties. High T_C superconductivity,^{7,8} colossal magnetoresistance,^{9,10} ferro-antiferro-nonmagnetic phenomena associated with exotic high-spin to low-spin magnetism,¹¹⁻¹³ metal-insulating transition,¹³⁻¹⁶ multifunctionality,^{17,18} piezochromism and piezomagnetism,^{19,20} or extreme polymorphism such as the perovskite-postperovskite transition at high pressure,²¹ are selected physical phenomena, which are induced by subtle structural changes around the transition-metal ion (M). The prediction of whether compression of AMX_3 and A_2MX_4 perovskites yields MX_6 tilting or it favors $M-X-M$ bond alignment toward an ideal perovskite still remains a subject of strong controversy.²²⁻²⁵ Nevertheless, this knowledge is crucial in explaining and eventually predicting high-pressure high-temperature structures and their associated properties. In addition, it is worthwhile in tailoring materials whose electronic properties rely on a delicate balance between the competing magnetic interactions involving e_g and t_{2g} orbitals of M , and p orbitals of X: O, F, or Cl. The $M-X-M$ bond angle between ad-

acent octahedra is a key structural parameter modulating both crystal structure and electronic properties. Moreover, a perovskite under compression can behave differently if compression is attained in a compound series (chemical pressure)²⁶⁻²⁸ or by applying external pressure.^{15,22,29} Although *ab initio* calculations have considerably increased the prediction capability of structural transformations under pressure to a considerable extent,⁶ the problem of how a network of interlinked MX_6 octahedra will evolve upon compression is subtle, deserving both experimental and theoretical feedback, and it still represents a major challenge in condensed-matter physics.

The system complexity increases if the MX_6 octahedra involve orbitally degenerate transition-metal ions (M : Cu^{2+} , Cr^{2+} , Fe^{2+} , Mn^{3+} , Ni^{3+} , or Co^{3+}). The Jahn-Teller (JT) coupling induces low-symmetry MX_6 distortions which are eventually responsible for the striking properties related to both the orbital ordering and JT distortion.

Based on the high compressibility of chloride layer perovskites, we report a structural study in the A_2CuCl_4 series (A: Rb, $\text{C}_n\text{H}_{2n+1}\text{NH}_3$; $n = 1-3$) as a function of both chemical and external pressure. The results will be extrapolated to other less compressible oxides and fluorides. We carried out x-ray diffraction (XRD), x-ray absorption (XAS), and optical absorption in the series. These measurements altogether

TABLE I. Structural parameters for $A_2\text{CuCl}_4$ ($A = \text{Rb}, \text{C}_n\text{H}_{2n+1}\text{NH}_3; n = 1-3$). R_{layer} and $R_{\text{Cu-Cu}}$ are the interlayer and the intralayer Cu-Cu distances, respectively. $R_{\text{ax}}, R_{\text{eq}}$, and Q_θ (all distances are given in Å) are the axial and equatorial Cu-Cl bond lengths and the tetragonal normal coordinate, respectively. The crystal bulk modulus K_0^C has been determined by fitting in the low-pressure range to a Murnaghan's equation of state from $V(P)$ data obtained by x-ray diffraction.

A	V (Å ³)	$R_{\text{Cu-Cu}}$	R_{layer}	R_{ax}	R_{eq}	Q_θ	K_0^C (GPa)
Rb	803.5	5.09	7.77	2.72	2.35	0.43	20
CH_3NH_3	999.0	5.18	9.33	2.91	2.28	0.71	
$\text{C}_2\text{H}_5\text{NH}_3$	1162.9	5.24	10.59	2.98	2.28	0.80	8.4
$\text{C}_3\text{H}_7\text{NH}_3$	1382.8	5.30	12.33	3.04	2.29	0.87	7.1

provide the crystal structure, space group, and local structure of the CuCl_6 octahedron (Cu-Cl bond lengths), and the energy of the d orbitals (crystal-field strength, e_g-t_{2g} splittings, and JT energy).

The $A_2\text{CuCl}_4$ structure at ambient conditions (Table I) indicates that CuCl_6 shows an elongated distortion of mainly tetragonal symmetry (Fig. 1). The associated distortion, expressed in terms of two-long (R_{ax}) and four-short (R_{eq}) Cu-Cl bond distances through the normal coordinate $Q_\theta = \frac{2}{\sqrt{3}}(R_{\text{ax}} - R_{\text{eq}})$, decreases with chemical pressure from 0.87 to 0.43 Å on passing from $(\text{C}_3\text{H}_7\text{NH}_3)_2\text{CuCl}_4$ ($V = 1382.8$ Å³) to Rb_2CuCl_4 ($V = 803.5$ Å³). The large volume reduction is mainly governed by the A -cation size since the corresponding

interlayer distance R_{layer} varies from 12.33 to 7.77 Å, whereas the intralayer Cu-Cu distance $R_{\text{Cu-Cu}}$ only varies from 5.30 to 5.09 Å, respectively.

To a great extent, layers of interconnected CuCl_6 octahedra are preserved along the series, the interlayer separation being the most affected. The strong Q_θ decrease with chemical pressure in comparison to $R_{\text{Cu-Cu}}$ is due to a drastic reduction of the apical in-plane Cu-Cl bond length R_{ax} toward a nearly O_h symmetry, i.e., shared Cl atoms move into a midway position on the Cu-Cl-Cu bond as $R_{\text{Cu-Cu}}$ decreases (Fig. 1). The suppression of the in-plane JT-induced orbital ordering (antiferrodistortive structure) will occur if $R_{\text{ax}} \approx R_{\text{eq}}$. Although this scenario has often been employed to explain the $A_2\text{CuCl}_4$ pressure behavior,³⁰ here we demonstrate that CuCl_6 compresses differently upon chemical and external pressure due to the unexpectedly similar compressibility $R_{\text{Cu-Cu}}$ and R_{layer} . XRD and XAS experiments under pressure performed in $(\text{C}_3\text{H}_7\text{NH}_3)_2\text{CuCl}_4$, $(\text{CH}_3\text{NH}_3)_2\text{CuCl}_4$ and Rb_2CuCl_4 (Figs. 2 and 3), together with XRD data on $(\text{C}_2\text{H}_5\text{NH}_3)_2\text{CuCl}_4$,³⁰ support this view. The cell volume reduces almost isotropically with hydrostatic pressure from 1400 to 1050 Å³ (around 25%) in $(\text{C}_3\text{H}_7\text{NH}_3)_2\text{CuCl}_4$ [from 1170 to 910 Å³ (22%) in $(\text{C}_2\text{H}_5\text{NH}_3)_2\text{CuCl}_4$] in the 0–6 GPa range. Likewise, $R_{\text{Cu-Cu}}$ and R_{layer} only vary from 5.3 to 4.9 Å (8%) [from 5.2 to 4.8 Å (8%)] and from 12.3 to 11.0 Å (11%) [from 10.6 to 10.0 Å (6%)] in the same pressure range, respectively, $(\text{C}_3\text{H}_7\text{NH}_3)_2\text{CuCl}_4$ being slightly more compressible and anisotropic than $(\text{C}_2\text{H}_5\text{NH}_3)_2\text{CuCl}_4$. Nevertheless, the pressure dependence of $R_{\text{ax}} + R_{\text{eq}}$ and $R_{\text{Cu-Cu}}$ is neatly different. Whereas $R_{\text{Cu-Cu}}$ reduces -0.4 Å from 0 to 6 GPa, $R_{\text{ax}} + R_{\text{eq}}$

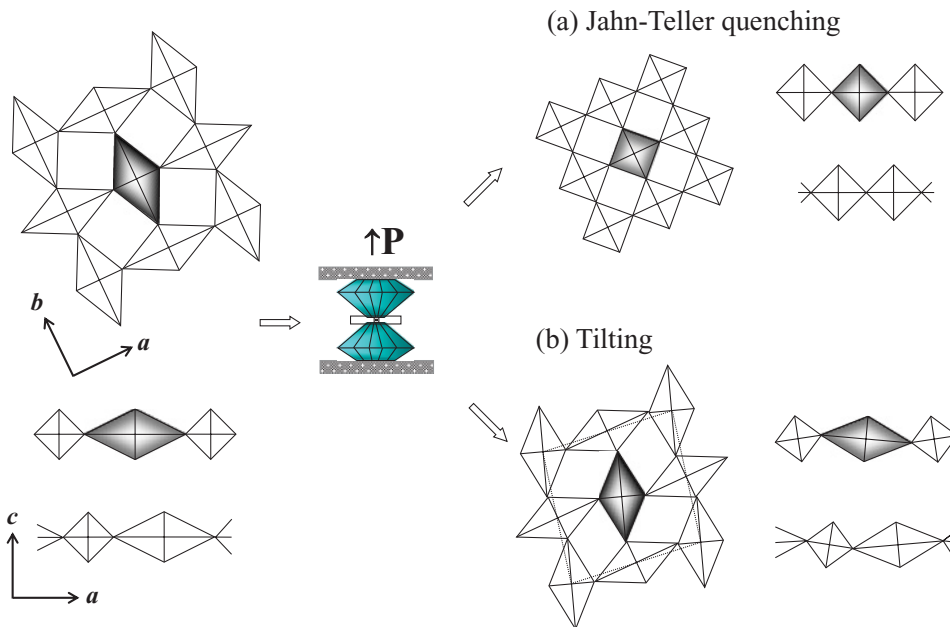


FIG. 1. (Color online) Left: Crystal structure of layered perovskites $A_2\text{CuCl}_4$ (orthorhombic $PbcA$), showing the in-plane (a), (b) antiferrodistortive structure displayed by the Jahn-Teller distorted CuCl_6 octahedra (top), and the interlayer structure along c (bottom). The CuCl_6 structure is given in terms of the tetragonal normal coordinate: $Q_\theta = \frac{2}{\sqrt{3}}(R_{\text{ax}} - R_{\text{eq}})$ (Table I). The rhombic normal coordinate along the series is $Q_\epsilon \approx 0$. Right: Extreme structural scenarios describing crystal transformation under pressure. (a) Ideal perovskite transformation yielding Jahn-Teller quenching (antiferrodistortive structure disappearance); (b) stability of the CuCl_6 Jahn-Teller distortion leading to pressure-induced tilts.

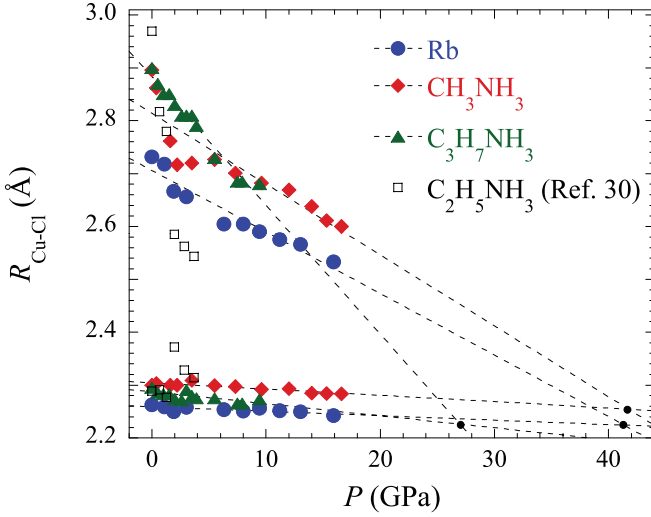


FIG. 2. (Color online) (a) Variation of the Cu-Cl bond lengths (R_{ax} and R_{eq}) of the D_{4h} elongated CuCl_6 with pressure in the $A_2\text{CuCl}_4$ layer perovskite series ($A = \text{Rb}, \text{C}_n\text{H}_{2n+1}\text{NH}_3; n = 1-3$) derived from x-ray absorption under pressure. The straight lines show the extrapolated P_{crit} for Jahn-Teller quenching ($R_{eq} = R_{ax}$). Note that P_{crit} is 27 and 41 GPa for $(\text{C}_3\text{H}_7\text{NH}_3)_2\text{CuCl}_4$, and $(\text{CH}_3\text{NH}_3)_2\text{CuCl}_4$ and Rb_2CuCl_4 , respectively. Bond lengths for $(\text{C}_2\text{H}_5\text{NH}_3)_2\text{CuCl}_4$ were obtained from x-ray diffraction data (Ref. 30).

decreases only -0.2 \AA in $(\text{C}_3\text{H}_7\text{NH}_3)_2\text{CuCl}_4$. A similar variation is also found in Rb_2CuCl_4 .

Note that both distances $R_{ax} + R_{eq}$ and $R_{\text{Cu-Cu}}$ and their pressure variation should coincide on the assumption of an ideal perovskite (in-layer Cu-Cl-Cu bond angle 180°). The observed distinct behavior and the fact that $|\delta R_{\text{Cu-Cu}}| > |\delta(R_{ax} + R_{eq})|$ clearly reveals pressure-induced CuCl_6 tilting. Moreover, the analogous variation of R_{ax} and R_{eq} with external pressure in the series means that CuCl_6 compresses similarly independently of the host crystal (Fig. 2).

The small local CuCl_6 compressibility, an order of magnitude less compressible than the bulk, explains why JT suppression in CuCl_6 can be barely detected below 20 GPa in layered perovskites. From $R_{ax}(P)$ and $R_{eq}(P)$ variations in Fig. 2, we conclude that a quasiregular CuCl_6 octahedron ($R_{ax} \approx R_{eq}$) would occur at about 30–40 GPa in $A_2\text{CuCl}_4$, depending on the crystal composition (i.e., A size). This finding contrasts with previous XRD results in $(\text{C}_2\text{H}_5\text{NH}_3)_2\text{CuCl}_4$,³⁰ reporting JT suppression quenching at the orthorhombic-to-monoclinic structural phase transition: $P_{crit} = 4 \text{ GPa}$. Suppression of the JT distortion at low pressures ($P_{crit} \leq 20 \text{ GPa}$) has also been reported for Mn^{3+} perovskites such as LaMnO_3 ,²⁹ $\text{Nd}_{0.5}\text{Ca}_{0.5}\text{MnO}_3$,³¹ and Ga-doped LaMnO_3 .³² The disparity of results providing different P_{crit} values must be ascribed to difficulties in obtaining reliable structural information from powder XRD in JT distortive materials. Structural studies under pressure in LaMnO_3 from XRD ($P_{crit} \approx 18 \text{ GPa}$),²⁹ XAS ($P_{crit} \approx 30 \text{ GPa}$),³³ Raman spectroscopy ($P_{crit} \approx 32 \text{ GPa}$),¹⁵ or *ab initio* calculations ($P_{crit} \approx 40 \text{ GPa}$)³⁴ illustrate such a controversy.

At this point we demonstrate that the knowledge of the JT energy E_{JT} associated with the low-symmetry distortion of the MX_6 octahedron can be decisive in order to estimate the criti-

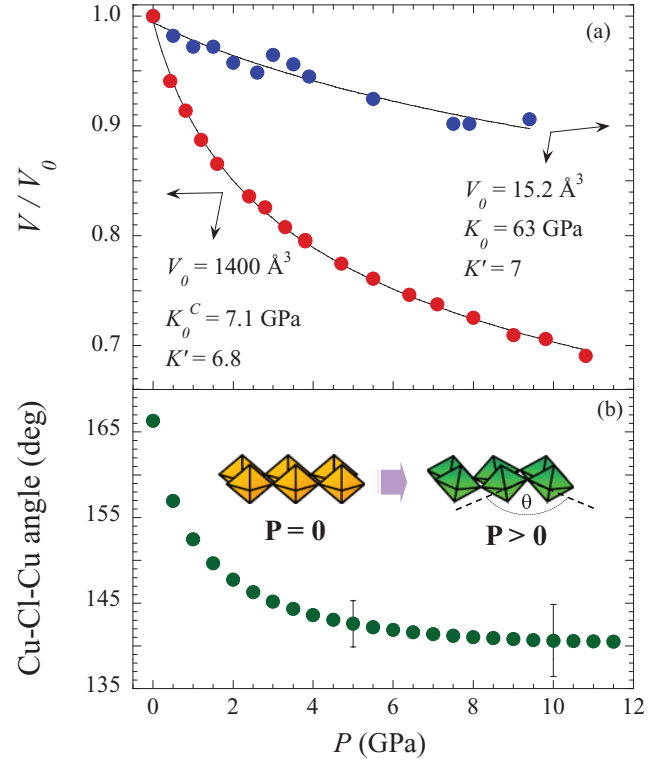


FIG. 3. (Color online) (a) Pressure dependence of $V(P)$ for the $(\text{C}_3\text{H}_7\text{NH}_3)_2\text{CuCl}_4$ crystal and CuCl_6 distorted octahedron. The lines correspond to least-square fits to a Murnaghan equation of state. The bulk modulus (K_0) and pressure derivative (K') are given for the crystal and octahedron. (b) Estimate of the in-layer Cu-Cl-Cu tilting angle with pressure in $(\text{C}_3\text{H}_7\text{NH}_3)_2\text{CuCl}_4$.

cal pressure for JT quenching. Particularly, it can be achieved for CuCl_6 since its electronic structure and hence E_{JT}/Cu^{2+} is known from optical absorption spectroscopy.³⁵ According to JT theory, the energy of the $a_{1g}(3z^2) \rightarrow b_{1g}(x^2 - y^2)$ transition ($E_1 = 1.0-1.5 \text{ eV}$) in $A_2\text{CuCl}_4$ ($A = \text{Rb}, \text{C}_3\text{H}_7\text{NH}_3$)³⁵ is directly related to the JT energy as $E_{JT} \approx E_1/4 = 0.25-0.38 \text{ eV}/\text{Cu}^{2+}$. E_{JT} corresponds to the free energy associated with the stabilization of the CuCl_6 octahedron from O_h to axially elongated D_{4h} in $A_2\text{CuCl}_4$. Therefore the P_{crit} value, which is required to transform an initially JT-distorted CuCl_6 back into O_h , must overcome the energy mismatch E_{JT} . This pressure can be obtained through E_{JT} following the scenario described in Fig. 1 from the local equation of state:

$$\begin{aligned} E_{JT} &= - \int_{V_0}^{V_{crit}} P(V) dV \\ &= - \frac{K_0}{K'} \int_{V_0}^{V_{crit}} \left[\left(\frac{V}{V_0} \right)^{-K'} - 1 \right] dV \\ &= \frac{K_0 V_0}{K'} \left(\frac{x^{1-K'} - K'}{K' - 1} + x \right). \end{aligned} \quad (1)$$

Here we assume quasiadiabatic conditions $\delta Q \approx 0$ ($\Delta U \approx W$) and $x = V_{crit}/V_0$ is the local volume reduction ratio, with $V_0 = (4/3)R_{eq}^2 R_{ax}$ being the volume of the CuCl_6 distorted octahedron at ambient conditions, and $V_{crit} = (4/3)R_{eq}^3$, the

final volume of the regular octahedron. K_0 and K' are the local CuCl_6 bulk modulus and corresponding pressure derivative, respectively. Equation (1) was derived on the assumption of a Murnaghan's equation of state,³⁶ which accurately describes the experimental relation between P and V/V_0 at constant temperature in the 0–6 GPa range using values of $V_0 = 20.5 \text{ \AA}^3$, $K_0 = 63 \text{ GPa}$, $K' = 7$ for $(\text{C}_3\text{H}_7\text{NH}_3)_2\text{CuCl}_4$ (Fig. 3), and $V_0 = 18.5 \text{ \AA}^3$, $K_0 = 140 \text{ GPa}$, $K' = 7$ for Rb_2CuCl_4 .³⁷ This estimate is based on the assumption that the equation of state applies up to P_{crit} , what is appropriate if P_{crit} is much smaller than K_0 . Hence the energy associated with JT quenching ($V_{\text{crit}} = 16.0$ and 15.4 \AA^3 , respectively) must, according to spectroscopic data, be at least $E_{\text{JT}} = 0.35 \text{ eV}$. Taking values of $x = V_{\text{crit}}/V_0 = 0.78$ for $(\text{C}_3\text{H}_7\text{NH}_3)_2\text{CuCl}_4$ and $x = 0.83$ for Rb_2CuCl_4 , we obtain, from Eq. (1), $E_{\text{JT}} = 0.4 \text{ eV}$. Although this value may be slightly overestimated due to dissipative energy effects upon compression, it accounts fairly for the JT energy derived from optical absorption data. It must be noted that E_{JT} given by Eq. (1) would drastically decrease if we neglect tilting and assume the structural scenario of an ideal layer perovskite [Fig. 1(a)] such as that proposed for $(\text{C}_2\text{H}_5\text{NH}_3)_2\text{CuCl}_4$ with $P_{\text{crit}} = 4 \text{ GPa}$.³⁰ In such a case, the local bulk modulus obtained from XRD is $K_0 = 18 \text{ GPa}$,³⁰ and, consequently the calculated JT energy $E_{\text{JT}} = 0.12 \text{ eV}$ would be three times smaller than the spectroscopic E_{JT} .³⁵ This model, therefore, supports that JT suppression in CuCl_6 takes place at about 30–40 GPa according to the scenario of Fig. 1(b) and is consistent with the pressure-induced tilting shown in Fig. 3. Model predictions also support recent structure and spectroscopic studies in CuWO_4 .^{38,39} Although the strong CuO_6 JT distortion decreases with pressure by a factor 2 from ambient pressure to 9 GPa, it is still stable up to 40 GPa, in agreement with the spectroscopic JT energy $E_{\text{JT}} = 0.3 \text{ eV/Cu}^{2+}$.³⁹

Pressure-induced JT quenching has also been widely investigated in Mn^{3+} oxides and fluorides.^{15,19,29–34} Some controversial and often contradictory results now can be clarified in light of present model. Likewise, from Eq. (1) we can estimate P_{crit} in a general way as $P_{\text{crit}} \approx E_{\text{JT}}/\Delta V$,

provided that $\Delta V \ll V_0$, with $\Delta V = V_0 - V_{\text{crit}}$ being the JT-related volume reduction. This simpler formulation is advantageous for systems where the local equation of state is missing but E_{JT} and ΔV are known from absorption spectroscopy and XRD, respectively. Following this procedure in CsMnF_4 ($E_{\text{JT}} = 0.45 \text{ eV/Mn}^{3+}$; $\Delta V = 1.49 \text{ \AA}^3$),¹⁹ epidote $\text{Ca}_2(\text{Al,Fe,Mn})\text{Al}_2\text{Si}_3\text{O}_{12}(\text{OH})$ ($E_{\text{JT}} = 0.37 \text{ eV/Mn}^{3+}$; $\Delta V = 1.20 \text{ \AA}^3$),⁴⁰ and LaMnO_3 ($E_{\text{JT}} = 0.25 \text{ eV/Mn}^{3+}$; $\Delta V = 1.05 \text{ \AA}^3$),⁴¹ we estimate P_{crit} to be about 40–50 GPa. Mn^{3+} JT quenching was observed in CsMnF_4 through optical spectroscopy at 37 GPa,¹⁹ in agreement with present estimates. The model also supports the experimental value $P_{\text{crit}} \approx 30 \text{ GPa}$ obtained from XAS³³ and Raman¹⁵ in LaMnO_3 and is consistent with electronic structure⁴¹ and density-functional theory³⁴ calculations, reporting $E_{\text{JT}} = 0.25 \text{ eV/Mn}^{3+}$ and JT-distortion stability for MnO_6 above 40 GPa, respectively.

In conclusion, pressure reduces the MX_6 JT distortion for Cu^{2+} and Mn^{3+} in perovskite-type structures, although the critical pressure required to transform back into O_h must be $P_{\text{crit}} \geq 20 \text{ GPa}$, in agreement with structural models based on the JT energy ($E_{\text{JT}} \geq 0.20 \text{ eV/JT ion}$). In A_2CuCl_4 , the stability of the CuCl_6 octahedral distortion in an ample pressure range is consistent with the important JT energy per Cu^{2+} ion, $E_{\text{JT}} = 0.25\text{--}0.38 \text{ eV/Cu}^{2+}$, measured by absorption spectroscopy. The local CuCl_6 compressibility is about an order magnitude smaller than the crystal compressibility, making it tilt upon compression but preserving the JT distortion above 20 GPa. A similar conclusion applies to Mn^{3+} in oxides and fluorides regardless of system dimensionality, confirming the experimental results performed by simultaneous XRD and XAS and by optical spectroscopy.

Financial support from the Spanish Ministerio de Ciencia e Innovación (Grant No. MAT2008-06873-C02-01/MAT) is acknowledged. X-ray absorption and diffraction experiments were done at D11/LURE (Project PS203-01), and ID09A/ESRF (HS2159), respectively. The MALTA Consolider Ingenio 2010 program (CSD2007-00045) is also acknowledged.

*fernando.rodriquez@unican.es

¹Y. Tokura and N. Nagaosa, *Science* **288**, 462 (2000).

²J. S. Zhou and J. B. Goodenough, *Phys. Rev. Lett.* **94**, 065501 (2005).

³K. I. Kobayashi, T. Kimura, H. Sawada, K. Terakura, and Y. Tokura, *Nature (London)* **395**, 677 (1998).

⁴M. Imada, A. Fujimori, and T. Yoshinori, *Rev. Mod. Phys.* **70**, 1039 (1998).

⁵J. P. Brodholt, *Nature (London)* **407**, 620 (2000).

⁶A. R. Oganov, R. Martonak, A. Laio, P. Raiteri, and M. Parrinello, *Nature (London)* **438**, 1142 (2005).

⁷J. G. Bednorz and K. A. Müller, *Z. Phys. B* **64**, 180 (1986).

⁸J. Orenstein and A. J. Millis, *Adv. Supercond. Sci.* **288**, 468 (2000).

⁹Y. Moritomo, A. Asamitsu, H. Kuwahara, and Y. Tokura, *Nature (London)* **380**, 141 (1996).

¹⁰I. Solovyev, N. Hamada, and K. Terakura, *Phys. Rev. Lett.* **76**, 4825 (1996).

¹¹D. P. Kozlenko, N. O. Golosova, Z. Jiráček, L. S. Dubrovinsky, B. N. Savenko, M. G. Tucker, Y. Le Godec, and V. P. Glazkov, *Phys. Rev. B* **75**, 064422 (2007).

¹²I. Fita, R. Szymczak, R. Puzniak, A. Wisniewski, I. O. Troyanchuk, D. V. Karpinsky, V. Markovich, and H. Szymczak, *Phys. Rev. B* **83**, 064414 (2011).

¹³M. Lafkioti, E. Goering, S. Gold, G. Schtz, S. N. Barilo, S. V. Shiryayev, G. L. Bychkov, P. Lemmens, V. Hinkov, J. Deisenhofer, and A. Loidl, *New J. Phys.* **10**, 123030 (2008).

¹⁴J. L. García-Muñoz, M. Amboage, M. Hanfland, J. A. Alonso, M. J. Martínez-Lope, and R. Mortimer, *Phys. Rev. B* **69**, 094106 (2004).

¹⁵M. Baldini, V. V. Struzhkin, A. F. Goncharov, P. Postorino, and W. L. Mao, *Phys. Rev. Lett.* **106**, 066402 (2011).

¹⁶J. D. Fuhr, M. Avignon, and B. Alascio, *Phys. Rev. Lett.* **100**, 216402 (2008).

¹⁷Y. Tokunaga, N. Furukawa, H. Sakai, Y. Taguchi, and T. Arima, *Nat. Mater.* **8**, 558 (2009).

- ¹⁸G. Lawes, A. B. Harris, T. Kimura, N. Rogado, R. J. Cava, A. Aharony, O. Entin-Wohlman, T. Yildirim, M. Kenzelmann, C. Broholm, and A. P. Ramirez, *Phys. Rev. Lett.* **95**, 087205 (2005).
- ¹⁹F. Aguado, F. Rodríguez, and P. Núñez, *Phys. Rev. B* **76**, 094417 (2007).
- ²⁰F. Aguado, F. Rodríguez, R. Valiente, A. Señas, and I. Goncharenko, *J. Phys. Condens. Matter* **16**, 1927 (2004).
- ²¹S. Yakovlev, M. Avdeev, E. Sterer, Y. Greenberg, and M. Mezouar, *J. Solid State Chem.* **182**, 1545 (2009).
- ²²R. J. Angel, J. Zhao, and N. L. Ross, *Phys. Rev. Lett.* **95**, 025503 (2005).
- ²³M. W. Lufaso and P. M. Woodward, *Acta Crystallogr. B* **60**, 10 (2004).
- ²⁴T. Tohei, A. Kuwabara, T. Yamamoto, F. Oba, and I. Tanaka, *Phys. Rev. Lett.* **94**, 035502 (2005).
- ²⁵B. J. Kennedy, T. Vogt, C. D. Martin, J. B. Parise, and J. A. Hriljac, *J. Phys. Condens. Matter* **13**, L925 (2001).
- ²⁶Y. Natsume and I. Yamada, *J. Phys. Soc. Jpn.* **54**, 4410 (1985).
- ²⁷J. A. Alonso, J. M. Martínez-Lope, M. T. Casals, and M. T. Fernández-Díaz, *Inorg. Chem.* **39**, 917 (2000).
- ²⁸C. D. Martin, S. Chaudhuri, C. P. Grey, and J. B. Parise, *Am. Mineral.* **90**, 1522 (2005).
- ²⁹I. Loa, P. Adler, A. Grzechnik, K. Syassen, U. Schwarz, M. Hanfland, G. K. Rozenberg, P. Gorodetsky, and M. P. Pasternak, *Phys. Rev. Lett.* **87**, 125501 (2001).
- ³⁰K. Ohwada, K. Ishii, T. Inami, Y. Murakami, T. Shobu, H. Ohsumi, N. Ikeda, and Y. Ohishi, *Phys. Rev. B* **72**, 014123 (2005).
- ³¹A. Arulraj, R. E. Dinnebier, S. Carlson, M. Hanfland, and S. van Smaalen, *Phys. Rev. Lett.* **94**, 165504 (2005).
- ³²L. Malavasi, M. Baldini, D. di Castro, A. Nucara, W. Crichton, M. Mezouar, J. Blasco, and P. Postorino, *J. Mater. Chem.* **20**, 1304 (2010).
- ³³A. Y. Ramos, H. C. N. Tolentino, N. M. Souza-Neto, J. P. Itié, L. Morales, and A. Caneiro, *Phys. Rev. B* **75**, 052103 (2007).
- ³⁴G. Trimarchi and N. Binggeli, *Phys. Rev. B* **71**, 035101 (2005).
- ³⁵R. Valiente and F. Rodríguez, *Phys. Rev. B* **60**, 9423 (1999).
- ³⁶F. D. Murnaghan, *Proc. Natl. Acad. Sci. USA* **30**, 244 (1944).
- ³⁷F. Aguado, F. Rodríguez, R. Valiente, M. Hanfland, and J. P. Itié, *J. Phys. Condens. Matter* **19**, 346229 (2007).
- ³⁸J. Ruiz-Fuertes, *Chem. Mater.* **23**, 4220 (2011).
- ³⁹J. Ruiz-Fuertes, A. Segura, F. Rodríguez, D. Errandonea, and M. N. Sanz-Ortiz, *Phys. Rev. Lett.* (to be published).
- ⁴⁰R. G. Burns, *Mineralogical Applications of Crystal Field Theory* (Cambridge University Press, Cambridge, UK, 1993).
- ⁴¹G. Zampieri, M. Abbate, F. Prado, A. Caneiro, and E. Morikawa, *Physica B* **320**, 51 (2002).